Advanced Composite Materials
Publication details, including instructions for authors and subscription information:
http://www.tandfonline.com/loi/tacm20

Experimental Evaluation of the Damage Growth Restraining in 90° Layer of Thin-ply CFRP Cross-ply Laminates

Hiroshi Saito [a] , Hiroki Takeuchi [b] & Isao Kimpara [a]
[a] Research Laboratory for Integrated Technological Systems, Kanazawa Institute of Technology, Hakusan, Ishikawa 924-0838, Japan
[b] Sakai Ovex Co., Ltd., Fukui, Fukui 918-8530, Japan
Version of record first published: 17 Jul 2012.

To cite this article: Hiroshi Saito , Hiroki Takeuchi & Isao Kimpara (2012): Experimental Evaluation of the Damage Growth Restraining in 90° Layer of Thin-ply CFRP Cross-ply Laminates, Advanced Composite Materials, 21:1, 57-66

To link to this article: http://dx.doi.org/10.1163/156855112X629522

VSP

Advanced Composite Materials 21 (2012) 57–66

ADVANCED COMPOSITE MATERIALS
brill.nl/acm

Experimental Evaluation of the Damage Growth Restraining in 90° Layer of Thin-ply CFRP Cross-ply Laminates

Hiroshi Saito [a,*], **Hiroki Takeuchi** [b] **and Isao Kimpara** [a]

[a] Research Laboratory for Integrated Technological Systems, Kanazawa Institute of Technology, Hakusan, Ishikawa 924-0838, Japan

[b] Sakai Ovex Co., Ltd., Fukui, Fukui 918-8530, Japan

Received 25 July 2011; accepted 20 December 2011

Abstract

In this paper, a systematic and detailed observation was made of the crack extension behavior of thin 90° layers of cross-ply carbon fiber reinforced plastics (CFRP) laminates. The effect of ply thickness on the crack propagation mechanism was discussed with respect to the energy release rate of the intralaminar transverse crack, calculated using finite element analysis. In a laminate with a 40 μm-thick-ply, the crack gradually extended with increasing strain. Conversely, extreme crack extension was found at around 1.0% strain in a laminate with a standard thick ply. Based on the numerical analysis, the crack suppression effect is verified using a thin ply; the effect is apparently caused by a decrease in the energy release rate at the crack tip in the thin layer.

Keywords

CFRP, thin ply, transverse crack, cross-ply laminate, finite element analysis

1. Introduction

In laminates, the layer aligned in the direction perpendicular to the loading direction causes intralayer transverse cracks under smaller strains than the failure strain of the entire laminate. The initial strain of the transverse crack and the crack density in such a 90° layer reportedly increase with decreasing ply thickness [1–3]. Because transverse cracks cause interlaminar delamination, the suppression of transverse cracks is important in the design of materials.

Recently, Kawabe *et al*. [4–8] developed a tow-spreading technology with large-tow fiber bundles, such as 12 k or 24 k, to produce 40-μm-thick plies without any damage throughout the process. Thin-ply laminated composites can reportedly sup-

* To whom correspondence should be addressed. E-mail: hsaito@neptune.kanazawa-it.ac.jp
Edited by the JSCM

DOI:10.1163/156855112X629522

press microcracking and delamination without the use of special resins and/or 3-D reinforcements [6, 7, 9]. In addition, enhancements to the following mechanical properties of thin-ply laminates have been reported: (i) unnotched tension strength [6, 7, 10], (ii) open-hole tension strength [6, 7], (iii) open-hole compression strength [10] and (iv) fatigue life [6, 9, 10].

Even though there is a lot of work on the initiation and propagation of transverse cracks in laminates with standard thick layers [1–3, 11–18], there has been little research done on laminates with thin layers. Thus, the failure mechanism of thin-ply laminates remains unclear.

In this paper, the effect of ply thickness on the crack propagation mechanism is discussed. We conducted precise observations of the crack propagation behavior in cross-ply laminates with different ply thicknesses under a monotonic tensile load. The mechanism of crack propagation in a thin-ply laminate was discussed with respect to the energy release rate of the intralaminar transverse crack and calculated using finite element analysis.

2. Materials and Testing Methods

The thin-ply prepreg used for the 90° layer consisted of IMS60-24 k carbon fiber and epoxy resin. This prepreg was manufactured by the Sakai Ovex Co. Ltd. The ply thickness was about 40 μm. T700SC/#2592 prepreg (Toray Industries, Inc., ply thickness about 240 μm) was used for the 0° layer. The stacking sequence of the laminate was $[0°_2/90°_n/0°_2]$ ($n = 1$, 2 and 4); that is, the thickness of the 90° layer varied from 40 to 160 μm. In this paper, the laminate with the 40-μm-thick 90° layer was designated as '$n = 1$'. All laminates were molded in an autoclave.

The tensile test specimens were 200 mm in length and 2.5 mm in width. A schematic illustration is shown in Fig. 1. The thicknesses of the specimens were 1.00 mm for $n = 1$, 1.04 mm for $n = 2$, and 1.12 mm for $n = 4$. The gage length was 100 mm, and strain gages were glued on both sides of the specimen in the center of the gage region. For the crack propagation observations, the lateral faces of the specimens were polished using 1 μm diamond grains.

A tensile load was applied to the specimen by a servo-hydraulic testing machine (EHF-EB100 kN-20 L, 100 kN capacity, Shimadzu Co. Ltd.). The testing rate was 1 mm/min. We also conducted *in situ* observations of crack extension in the 90° layer. The numbers and lengths of the cracks were measured using a dig-

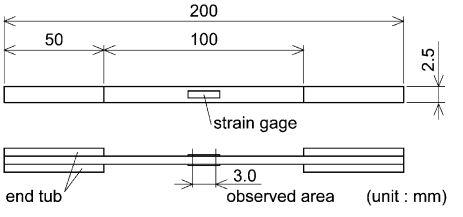

Figure 1. Dimensions of the specimen for crack extension observation.

ital microscope (VHX-500, Keyence Corporation). The microscope magnification was 1000–3000 times. The observation range was 3 mm in the center of the gage region. The examination was interrupted to observe the crack propagation at 0.1% strain intervals, while maintaining the load. The test was continued until the strain reached 1.5%. A countable transverse crack in this study is defined as follows: if the two debondings between a fiber and the matrix were connected to each other, these debondings were counted as a transverse crack.

3. Results and Discussions

3.1. Crack-propagation Observation Results

Figure 2(a) shows the crack extension in $n = 1$. At 0.4% strain, the debondings between fiber and matrix initiated. The opening displacement of these debondings increased with increasing strain. The debondings connected to each other and formed a transverse crack at 0.8% strain. However, the crack length increased as the strain increased, and the transverse crack did not perfectly penetrate the 90° ply until 1.5% strain.

Figure 3(a) shows the relation between the normalized crack length and the strain in $n = 1$. The crack extension tended to slow down when the normalized crack length reached approximately 0.75–0.80. Therefore, few specimens caused crack penetration in the 90° layer until the strain reached 1.5%.

Figure 2(b) shows the crack extension in $n = 2$. Similarly to $n = 1$, debondings were observed at 0.4% strain. Once a transverse crack forms at 1.0% strain, it rapidly propagates at about 1.1 and 1.3% strain. The transverse crack penetrated the 90° layer at 1.3% strain.

The relation between the normalized crack length and the strain is shown in Fig. 3(b). Crack extension was initiated at approximately 1.0% strain. Then, the crack completely penetrated the 90° layer at around 1.2% strain.

Figure 2(c) shows the crack extension in $n = 4$. Debondings between fiber and matrix were initiated at 0.7% strain. A transverse crack, which originated from these debondings, penetrated the 90° layer at 1.0% strain.

Figure 3(c) shows the relation between the normalized crack length and the strain in $n = 4$. Severe crack extension was initiated at approximately 1.0% strain. The crack length immediately reached the layer thickness of the 90° layer at 1.1% strain.

3.2. Crack Density and Crack-opening Displacement

Figure 4 shows the relation between the crack density and the strain for each ply thickness. The number of cracks was counted along the normalized crack length. In the case of $n = 1$, it was found that many cracks with a normalized length less than 0.75 were initiated at less than 1.0% strain. In contrast, in the cases of $n = 2$ and 4, most of the cracks at strains larger than 1.0% had a normalized length of 1.0; that is, the crack completely penetrated through the 90° layer.

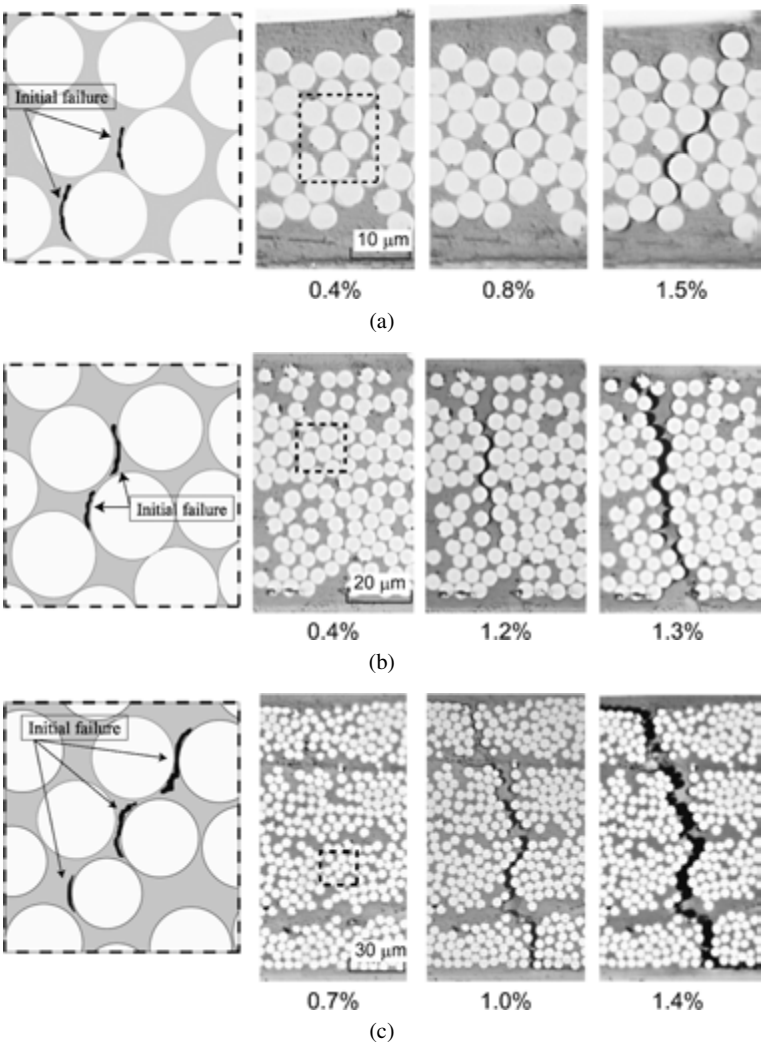

Figure 2. Observation results of crack extension in 90° layer. (a) $n = 1$ (ply thickness: 40 μm); (b) $n = 2$ (ply thickness: 80 μm); (c) $n = 4$ (ply thickness: 160 μm).

Figure 5 shows the relation between the crack-opening displacement (COD) and the strain. The COD was measured using a digital-image-processing technique at the largest opening region of the crack. The COD in $n = 1$ was much smaller than that in $n = 2$ and 4. It is supposed that the crack in the 90° layer in $n = 1$ was difficult to open because the stiff 0° layer was located nearby. The crack extension that followed the increase in COD leads to stress relaxation in the 90° layer. Conversely, for $n = 1$ it was difficult to cause stress relaxation in the 90° layer because the COD was very small. Therefore, the higher stress field maintained in the 90° layer caused new cracks around the existing cracks in $n = 1$, and the crack density became higher.

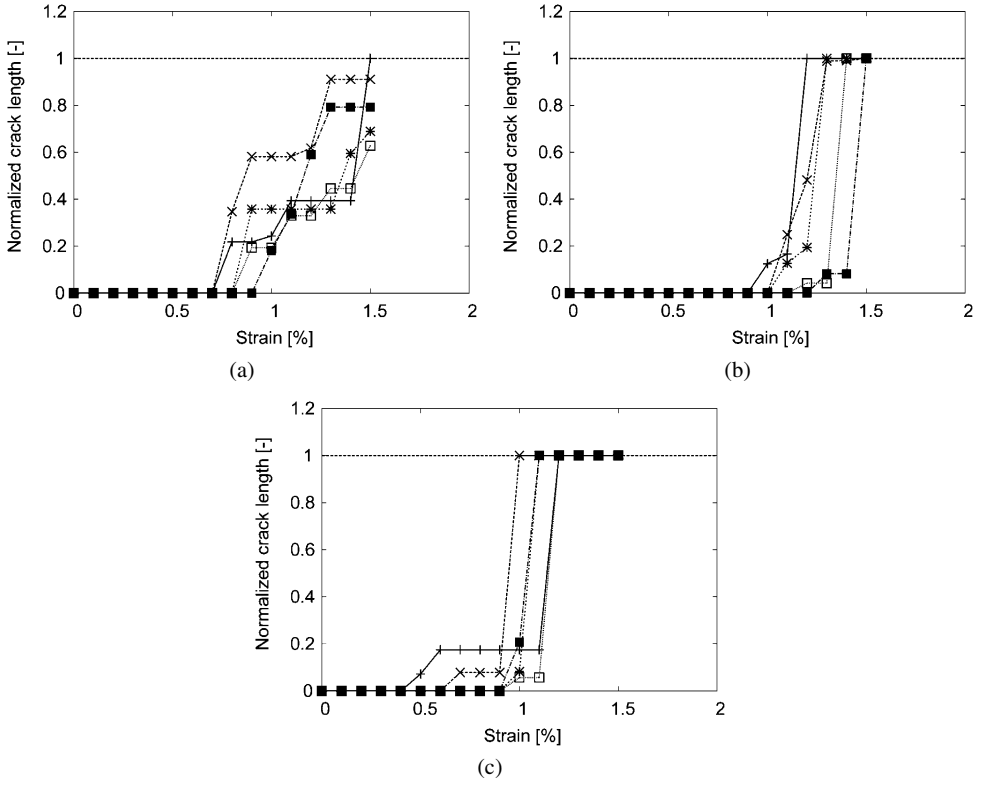

Figure 3. Relation between normalized crack length and strain. (a) $n = 1$ (ply thickness: 40 μm); (b) $n = 2$ (ply thickness: 80 μm); (c) $n = 4$ (ply thickness: 160 μm).

4. Discussion of Crack Extension Mechanism with Numerical Simulation

4.1. Numerical Simulation Model

From the observation results, in the case of $n = 1$, it was found that the crack gradually extended with increasing strain. In contrast, severe crack extension was observed at around 1.0% strain for $n = 2$ and 4. In this study, we focused on the energy release rate at the crack tip [20], and the effect of ply thickness on the crack extension behavior was evaluated using finite element (FE) analysis.

The FE analysis was conducted with the commercial software MSC. Marc 2008r1. Figure 6 shows a schematic illustration of the finite element model and its boundary conditions. This is a 2-D half model, symmetrical about the neutral plane. The eight-node isoparametric element was used. The numbers of elements and nodes were 2400 and 7755 for $n = 1$, 4000 and 12 587 for $n = 2$, and 7200 and 22 251 for $n = 4$. The 0° and 90° layers were represented as homogeneous materials. The materials properties used in this analysis are shown in Table 1. The thermal residual stress was also considered in the model. The applied temperature difference was 105°C. The thickness of the 90° layer varied from 40 to 160 μm. A transverse

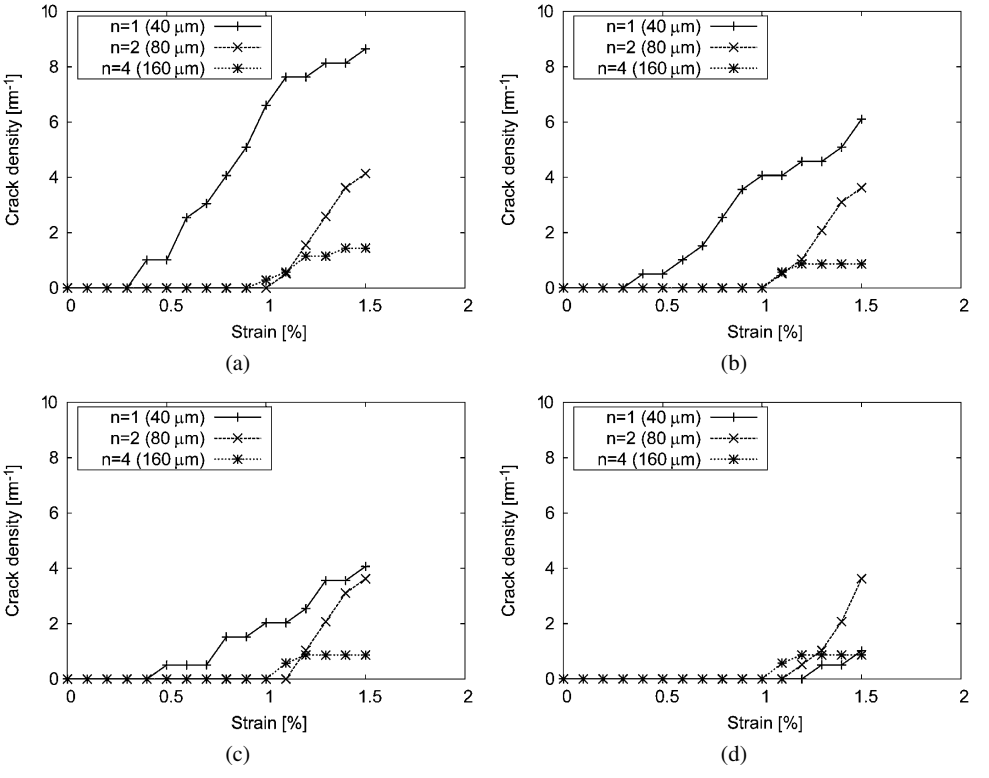

Figure 4. Relation between crack density and strain. (a) Normalized crack length > 0.25; (b) normalized crack length > 0.50; (c) normalized crack length > 0.75; (d) normalized crack length = 1.0.

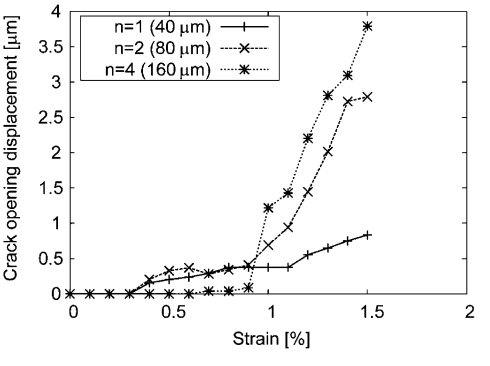

Figure 5. Relation between COD and strain.

crack was inserted in the 90° layer from the neutral plane. The crack was represented by the double nodes between the adjacent elements. The normalized crack length ranged from 0 to 1. In each crack length, we calculated the relation between the strain and the energy release rate at the crack tip.

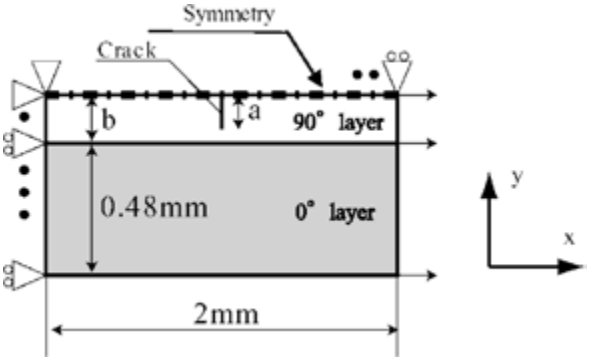

Figure 6. Schematic illustration of the finite element model.

Table 1.
Materials properties for finite element analysis

	Modulus E (GPa)	Poisson's ratio ν	Thermal expansion coefficient a ($\times 10^{-6}$/K)
0° layer	113.5	0.3	1.0
90° layer	8.31	0.45	22.5

4.2. Numerical Simulation Results

Figure 7 shows the contour figure of the energy release rate superimposed on the experimentally obtained crack extension results. It is obvious that the maximum energy release rate is at approximately 75% of the layer thickness at any strain. This trend apparently depends on the existence of the adjacent 0° layer, which has much higher stiffness than the 90° layer.

In the cases of $n = 2$ and $n = 4$, severe crack extension was observed around 1.0% strain, as mentioned above. At this strain, it is found that the energy release rate was approximately 20 to 40 J/m^2 in both $n = 2$ and $n = 4$. In contrast, the maximum energy release rate marginally reached the range between 20 and 40 J/m^2 at 1.4% strain in the case of $n = 1$, in which most of the cracks gradually extended through the 90° layer. Therefore, a range of energy release rate between 20 and 40 J/m^2 appears to be the threshold for severe crack propagation. This energy release rate for severe crack extension corresponds well with the results obtained by other researchers [18, 19]. Yokozeki *et al*. [18] evaluated the damage process for transverse cracking in 90° plies under static loading using cross-ply and quasi-isotropic CFRP laminates. They calculated the energy release rate associated with crack propagation using three-dimensional FE models and obtained a value of about 40 J/m^2. Pegoretti *et al*. [19] calculated the energy release rate at crack initiation between epoxy and E-glass single fibers, and they obtained a value of approximately 33 J/m^2. Therefore, it is concluded that a crack suppression effect exists, and is

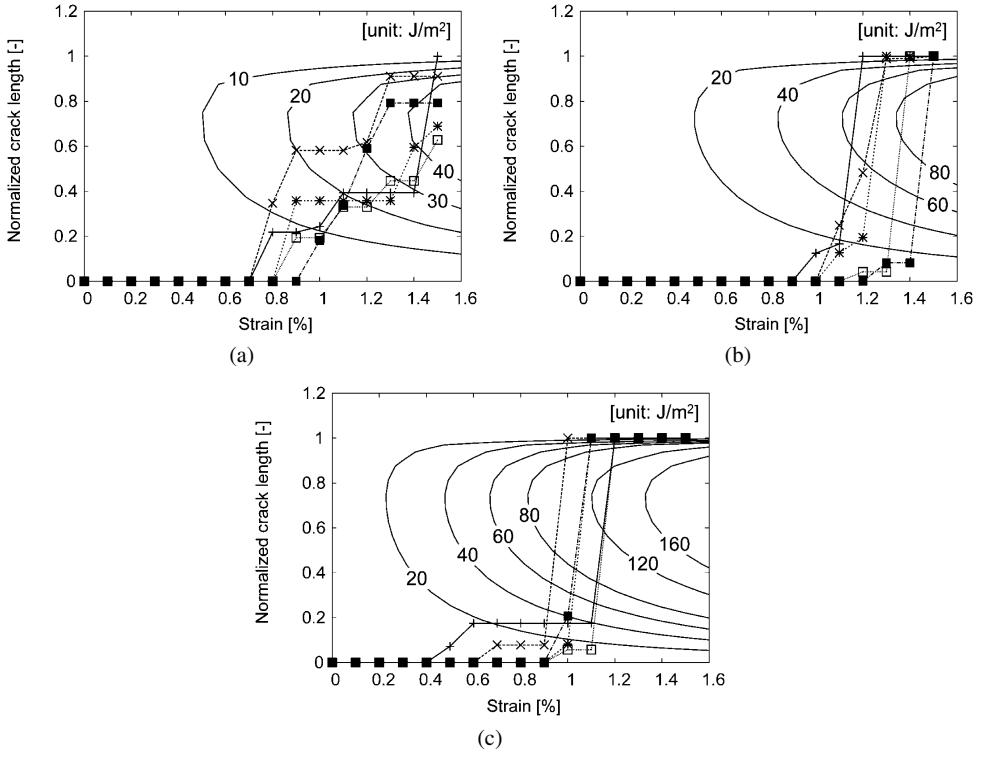

Figure 7. Contour figures of energy release rate superimposed on the experimental results. (a) $n = 1$ (ply thickness: 40 μm); (b) $n = 2$ (ply thickness: 80 μm); (c) $n = 4$ (ply thickness: 160 μm).

supposedly caused by a decrease in the energy release rate at the crack tip in a thin layer.

5. Conclusions

In this paper, we discussed the effects of ply thickness on the crack propagation mechanism. We conducted precise observations of the crack propagation behavior in cross-ply laminates with different ply thicknesses under a monotonic tensile load. The mechanism of crack propagation in a thin-ply laminate was discussed with respect to the energy release rate of the intralaminar transverse crack, calculated using finite element analysis. The results are summarized as follows.

1. In the case of $n = 1$, the transverse crack gradually extended with increasing strain, and did not perfectly penetrate the 90° ply until 1.5% strain. In contrast, severe crack extension was observed at around 1.0% strain in $n = 2$ and 4.

2. In the case of $n = 1$, many cracks with normalized length less than 0.75 started at less than 1.0% strain. The crack completely penetrated through the 90° layer in $n = 2$ and 4. The COD in $n = 1$ was much smaller than that in $n = 2$ and 4. It

is thought that the crack in the 90° layer in $n = 1$ was difficult to open because of the close proximity of the stiff 0° layer.

3. From the results of the finite element analysis, it was found that the energy release rate was approximately 20 to 40 J/m^2 in both $n = 2$ and 4. In contrast, the maximum energy release rate marginally reached the range 20–40 J/m^2 at 1.4% strain in the case of $n = 1$. Therefore, a range of energy release rate values between 20 and 40 J/m^2 appears to be the threshold for severe crack propagation.
4. The crack suppression effect exists and was verified using a thin ply; the effect is supposedly caused by a decrease in the energy release rate at the crack tip in the thin layer.

References

1. A. Parvizi and J. E. Bailey, On multiple transverse cracking in glass fibre epoxy cross-ply laminates, *J. Mater. Sci.* **13**, 2131–2136 (1978).
2. K. W. Garrett and J. E. Bailey, Multiple transverse fracture in 90° cross-ply laminates of a glass fibre-reinforced polyester, *J. Mater. Sci.* **12**, 157–168 (1977).
3. S. Ogihara, N. Takeda and A. Kobayashi, Experimental characterization of microscopic failure process under quasi-static tension in interleaved and toughness-improved CFRP cross-ply laminates, *Compos. Sci. Technol.* **57**, 267–275 (1997).
4. K. Kawabe, S. Tomoda and T. Matsuo, A pneumatic process for spreading reinforcing fiber tow, in: *42nd Intl SAMPE Sympos. Exhibit.*, Anaheim, CA, USA, May 4–8, pp. 65–76 (1997).
5. H. Sasayama, K. Kawabe, S. Tomoda, I. Ohsawa, K. Kageyama and N. Ogata, Effect of lamina thickness on first ply failure in multidirectionally laminated composites, in: *8th Japan Intl SAMPE Sympos. Exhibit. (JISSE-8)*, Tokyo, Japan, pp. 18–21 (2003).
6. S. W. Tsai, S. Sihn and R. Y. Kim, Thin ply composites, in: *Collection of Technical Papers — AIAA/ASME/ASCE/AHS/ASC Struct.*, *Struct. Dynam. Mater. Conf.*, Vol. 4, AIAA/ASME/ASCE/AHS/ASC, Austin, TX, USA, pp. 2555–2559 (2005).
7. S. Sihn, R. Y. Kim, K. Kawabe and S. W. Tsai, Experimental studies of thin-ply laminated composites, *Compos. Sci. Technol.* **67**, 996–1008 (2007).
8. K. Kawabe, H. Sasayama and S. Tomoda, New carbon fiber tow-spread technology and applications to advanced composite materials, *SAMPE J.* **45**, 6–17 (2009).
9. Y. Nishikawa, K. Okubo, T. Fujii and K. Kawabe, Fatigue crack constraint in plain-woven CFRP using newly-developed spread tows, *Intl J. Fatigue* **28**, 1248–1253 (2006).
10. T. Yokozeki, Y. Aoki and T. Ogasawara, Experimental characterization of strength and damage resistance properties of thin-ply carbon fiber/toughened epoxy laminates, *Compos. Struct.* **82**, 382–389 (2008).
11. F. W. Crossman, W. J. Warren, A. S. D. Wang and G. E. Law, Initiation and growth of transverse cracks and edge delamination in composite laminates, Part 2. Experimental correlation, *J. Compos. Mater.* **14**, 88–108 (1980).
12. A. S. D. Wang and F. W. Crossman, Initiation and growth of transverse cracks and edge delamination in composite laminates, Part 1. An energy method, *J. Compos. Mater.* **14**, 71–87 (1980).
13. A. S. D. Wang, N. N. Kishore and C. A. Li, Crack development in graphite–epoxy cross-ply laminates under uniaxial tension, *Compos. Sci. Technol.* **24**, 1–31 (1985).

14. L. Boniface, P. A. Smith, M. G. Bader and A. H. Rezaifard, Transverse ply cracking in cross-ply CFRP laminates — initiation or propagation controlled? *J. Compos. Mater.* **31**, 1080–1112 (1997).
15. N. Takeda and S. Ogihara, *In situ* observation and probabilistic prediction of microscopic failure processes in CFRP cross-ply laminates, *Compos. Sci. Technol.* **52**, 183–195 (1994).
16. S. Ogihara and N. Takeda, Interaction between transverse cracks and delamination during damage progress in CFRP cross-ply laminates, *Compos. Sci. Technol.* **54**, 395–404 (1995).
17. N. Pagano, G. A. Schoeppner, R. Kim and F. L. Abrams, Steady-state cracking and edge effects in thermo-mechanical transverse cracking of cross-ply laminates, *Compos. Sci. Technol.* **58**, 1811–1825 (1998).
18. T. Yokozeki, T. Aoki and T. Ishikawa, Transverse crack propagation in the specimen width direction of CFRP laminates under static tensile loadings, *J. Compos. Mater.* **36**, 2085–2099 (2002).
19. A. Pegoretti, M. L. Accorsi and A. T. Dibenedetto, Fracture toughness of the fibre–matrix interface in glass–epoxy composites, *J. Mater. Sci.* **31**, 6145–6153 (1996).
20. J. Noda, T. Okabe, N. Takeda and M. Shimizu, Damage process of GFRP cross-ply laminates, *Trans. Japan Soc. Mech. Engng, Part A* **70**, 1364–1369 (2004) (in Japanese).